Silicon Particle Growth in a Fluidized-Bed Reactor

This paper describes the overall operation of a 15 cm dia. fluidized-bed reactor for silicon production via silane pyrolysis. The fluidized-bed reactor has been characterized by its performance data and parametric effects. A withdrawal system is used to selectively remove big particles. Seed generation is provided by a fluid jet milling device, which avoids metallic grinding contamination. The silicon particle size growth calculated from a scavenging/deposition model agrees with actual size measurements.

George Hsu, Naresh Rohatgi, John Houseman
Jet Propulsion Laboratory
California Institute of Technology
Pasadena, CA 91109

Introduction

In a conventional Siemens reactor, silicon is deposited heterogeneously on a hot filament through chemical vapor deposition by the hydrogen reduction of trichlorosilane. A coherent and dense silicon rod of semiconductor purity is obtained as the product. In this mode of operation, homogeneous decomposition is suppressed by limiting the trichlorosilane feed to a low concentration (<5%). As another deposition method, silane can be homogeneously pyrolyzed in a free-space reactor to yield very fine and light powders of submicron size. Even though the throughput is large due to high silane concentration, the powdery product has an extremely high surface area, which can lead to easy contamination, and has too low a density for handling. In between these two modes of operation, silane pyrolysis in a fluidized bed produces deposition on silicon seed particles. The resulting particle grows via heterogeneous chemical vapor deposition as well as via scavenging of homogeneous silicon nuclei due to the bouncing of particles back and forth in a fluidized bed. This leads to a high deposition rate as a combination of heterogeneous and homogeneous decomposition. Also, the throughput of silicon product can be high, as there is no critical silane limitation for excessive homogeneous fines formation, which would result from homogeneous nucleation without scavenging. Therefore, fluidized-bed silicon deposition represents a high-throughput, low-cost technology that is under active development as a potential replacement for the Siemens technology. This paper covers chemical engineering characterization of the reactor system, including the new devices for product withdrawal and seed generation, and illustrates the reactor system performance in terms of silicon particle growth. Current work includes inserting a quartz liner into the stainless steel reactor to ensure a product of low impurity. Product purity data for the quartz-lined reactor will be reported in future papers.

In a fluidized-bed reactor (FBR), silane is pyrolyzed and the released silicon is deposited on seed particles. Product particles of larger sizes are preferentially withdrawn from the boot located at the bottom of the reactor. A small portion of the product is ground into seeds via a seed generation device. The make-up seed particles are introduced into the reactor semicontinuously. The long-term engineering and cost requirements for the frequency and operation of the semicontinuous process are not considered in this paper. The recycle of make-up seed particles is not performed in the current reactor study. The mechanism for silicon particle growth and silane pyrolysis in a fluidized bed has been discussed previously (Hsu et al., 1984b; Rohatgi et al., 1982), and product characterization was reported in the literature (Hsu et al., 1984a, b; Rohatgi and Hsu, 1983).

Reactor System Design Considerations

The FBR is depicted in Figure 1. It is constructed from a nominal 15 cm schedule 40 stainless steel 316 pipe and has dimensions of 15.41 cm ID × 121.92 cm high. It has an expanded head of 60.96 cm × 60.96 cm to allow entrained particles to drop back into the bed.

Four essential factors affecting particle size in a fluidized-bed silicon production system are fluidization mode, temperature distribution, product withdrawal, and seed generation. They are controlled by four elements: distributor, heaters, withdrawal boot, and seed generation device. Their design considerations are discussed first; the overall reactor system performance relative to particle growth is then described.

Gas distributor

Five different types of gas distributors were investigated in this work:

- A porous carbon unit with nine spouts (Lackey and Sease, 1975)

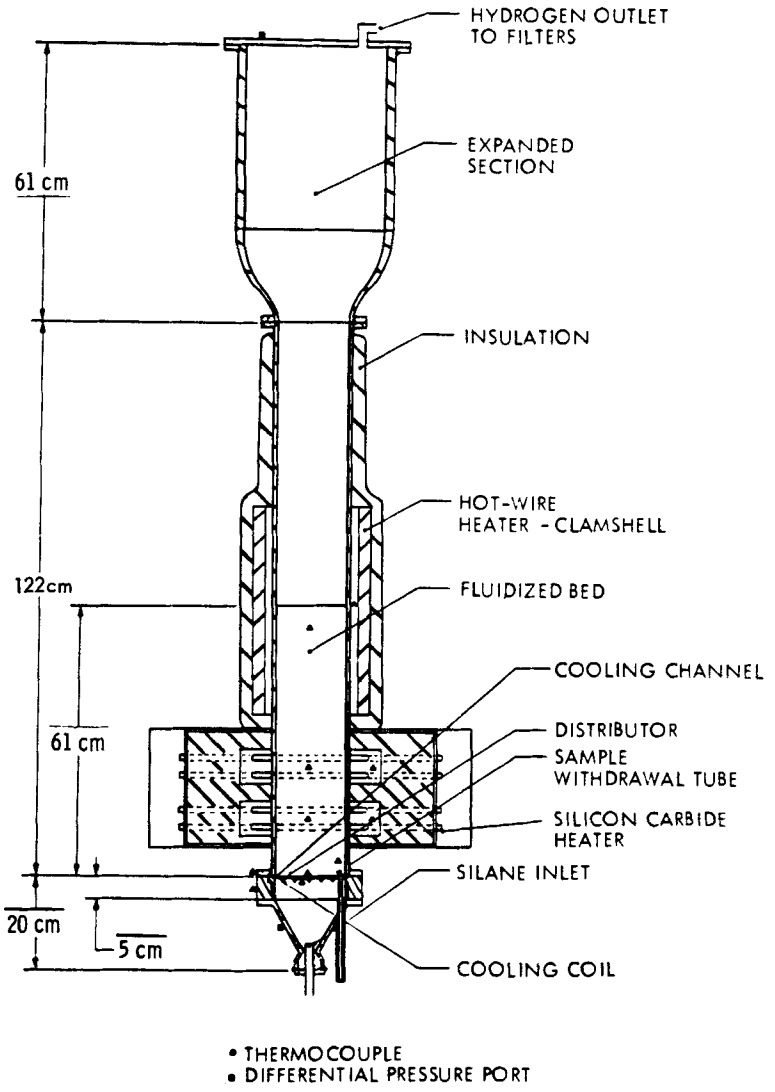

Figure 1. 15 cm dia. fluidized-bed reactor.

- A nozzle with 0.64 cm dia. opening
- A multilayer screen (Dynapore) distributor
- Two distributors fabricated from either one or two layers of 325 mesh stainless steel screen supported by a 0.127 cm thick plate perforated with 0.32 cm dia. holes

All these gas distributors were able to provide a bubbling fluidized bed with the exception of the nozzle-type distributor. Although a spouting distributor creates vigorous mixing of solids, it is difficult to ensure a firm contact of the metallic cooling coil underneath the porous carbon material. Distributors with one or two layers of 325 mesh screens were found most effective because of the simplicity in design to provide external water cooling.

The key to successful operation of the FBR is to keep the distributor temperature below 350°C. A distributor temperature above 350°C will cause partial decomposition of silane at the distributor, followed by clogging of the particles in the fluidized bed. Three distributor cooling systems were investigated:

1. Water cooling at the periphery of the distributor and a ½ in. (1.3 cm) thick cooling ring located between the distributor and the reactor flange
2. The same cooling system supplemented with internal water cooling tubes within the fluidized bed, located 0.64 cm above the distributor screen and
3. Water cooling at the periphery of the distributor in addition to a water cooling coil located beneath the distributor

A copper cooling coil was silver soldered to a 0.127 cm thick plate with multiple holes. The distributor screen is spot welded to the support plate to ensure firm contact. The first two cooling systems were inadequate to keep the distributor temperature below 350°C. The water cooling tubes located within the fluidized bed not only increased the load on the heaters but also caused an excessive temperature gradient between the fluidized bed and the reactor wall, resulting in silicon deposits on the wall. The third cooling system was found most satisfactory, both to keep the distributor temperature below 350°C and to eliminate deposits of silicon on the reactor wall.

Heaters

The FBR was externally heated. Under adiabatic conditions the minimum power, Q_H, required for the heater was calculated

as follows:

$$Q_H = \eta_1 \int_{T_{in}}^{T_{Bed}} C_{p_1}\, d_T + Q_w - \eta_{1\Delta H_R} \qquad (1)$$

The pyrolysis of silane is a mildly exothermic reaction with a ΔH_R of -5 kcal/mol (-20.95 kJ/mol). In order to keep the distributor temperature below 350°C to avoid premature decomposition of silane, the heat resulting from the impact of hot silicon particles on the distributor plate, Q_w, is removed by water cooling. The estimated minimum heater output required to heat 3 mol/min of silane in a FBR from 300 to 973K is 4 kW. The bottom silane inlet portion of the FBR is heated by a two-zone, fast-response, 30 cm high silicon carbide heater with a total output of 9 kW. Both zones are independently controlled in order to achieve an isothermal condition in the bed within 7.6 cm from the distributor, Figure 2. On the top of the silicon carbide heater there is a single-zone, independently controlled 45.7 cm high ceramic clamshell heater with a total power output of 9 kW. The main purpose of this heater is to provide thermal insulation around the reactor and distribute the heat input throughout the bed height. This helps keep the temperature difference between the reactor wall and the bed small (within 100°C). Thus, in order to heat the bed silicon to 650°C, lower temperatures will be required to be kept on the reactor wall side. This will minimize risk of deposition of silicon on the reactor wall.

Product withdrawal system

The fluidized-bed reactor is equipped with a continuous silicon withdrawal system to maintain a constant bed height in the reactor. It is designed to withdraw silicon particles at a rate of up to 3 kg/h. This system is depicted in Figure 3. It consists of an externally water-cooled silicon withdrawal tube, 38 cm long × 2.2 cm ID. The particles in the silicon withdrawal tube

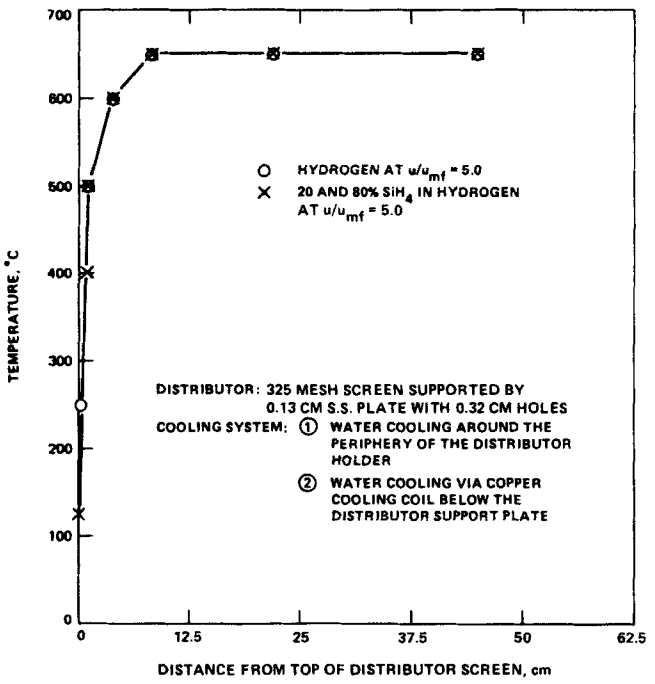

Figure 2. Axial temperature profile in fluidized-bed reactor from entrance.

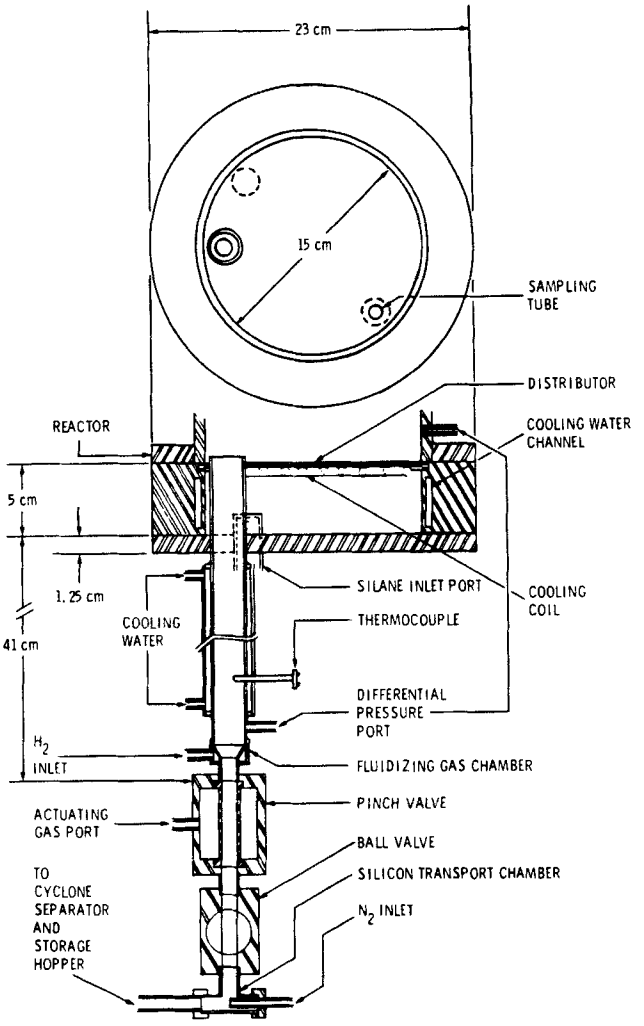

Figure 3. Product withdrawal system—a reactor separation boot.

were mildly fluidized at a u/u_{mf} of one in order to:

1. Keep silane out of the withdrawal tube
2. Permit accumulation of large particles in the tube
3. Cool the tube more effectively by preventing a sudden drop of hot bed particles within the tube.

An electronically controlled pinch valve (Red Valve) is located at the bottom of the tube. This valve is opened at a predetermined frequency (10–15 s intervals) for a duration of 1 s to allow particles to drop into a tee. The tube is water-cooled and provides cooling for the particles. The particles in the tee are pneumatically transported to a cyclone separator and collected in a silicon holding tank.

Seed generation device

The prior technique for preparing fluidized bed seed involved grinding semiconductor-grade silicon, followed by leaching with acids. Not only are these efforts tedious and costly, they tend to introduce metallic contaminants through grinding. A jet milling technique to grind silicon by impinging jets is being studied in this work for seed particle generation. Specifically, this device involves grinding silicon particles by the impingement of two opposing nitrogen jets carrying silicon particles. The device and

its dimensions are shown in Figure 4. It is lined with high-density polypropylene to avoid exposure of the silicon to metallic surfaces.

Reactor System Performance

Operation characterization

A total of 29 runs were conducted to evaluate the reactor performance and parametric effects. The temperature of the bed was generally maintained at 650 to 700°C. Some experiments were conducted at 450 to 550°C bed temperature, which yielded incomplete conversion of silane. The silane conversion efficiency was almost 100% at 650°C bed temperature.

An experiment was conducted during which the silane concentration was varied from 20 to 100% in hydrogen to determine the upper limit of concentration of silane that can be fed into a fluidized-bed reactor. Each silane concentration was maintained for at least 15 min, during which a silicon bed sample and a dust sample at the filter were collected. With an increase in silane concentration from 20 to 100%, the fines in the effluent increased from 0.85 to 6%, as measured by the effluent sample filter. The overall dust formation for the entire run includes three portions:

1. The majority, the fines in the effluent mentioned above
2. A minor amount of dust adhered on the surface of reactor expansion section
3. A portion of the homogeneously nucleated fines retained in the bed (smaller than the original seed) as measured by the sieve analysis of product after run.

The maximum overall dust formation was 9.5% at a silane concentration of 57%. The ability of the FBR to accept up to 100% feed silane concentrations without producing excessive dust or bed agglomeration is a great advantage. Not only does it simplify the process design, it also results in an increased production rate.

Results shows that more than 90% of the silicon feed as silane was retained in the bed as deposited material and less than 10% was collected in the filter as fines elutriants. With an increase in feed silane concentration from 20 to 80%, the rate of silicon product increases from 0.9 to 3.5 kg/h. In order to produce 100 metric tons (MT) per year of silicon, at a production rate of 3.5 kg per reactor-hour and a 70% on-stream time factor, five fluidized-bed reactors of 15 cm dia. are needed. In a commercial Siemens process, silicon is produced strictly by heterogeneous decomposition of trichlorosilane on a deposition rod. For a Siemens bell jar reactor of 50 cm dia. × 1.2 m high, a typical product rate is 0.5 kg/h. In order to produce the same 100 MT/yr of silicon, one would need 33 bell jar reactors, compared to only five 15 cm fluidized-bed reactors.

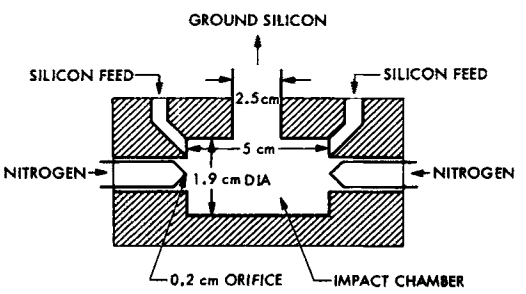

Figure 4. Jet milling device for fluidized-bed seed particle generation.

The fluidization mode of bed particles is characterized by a gas velocity ratio u/u_{mf} (Kunii and Levenspiel, 1969), where u is the superficial gas velocity and u_{mf} is the minimum fluidization velocity. The operating limits for bubbling fluidized-bed silane pyrolysis were previously identified as $3 \leq u/u_{mf} \leq 8$ (Hogle et al., 1978, Rohatgi et al., 1982; Hsu et al., 1984a, b). At $u/u_{mf} \leq 3$, long residence time in a local reaction zone results in high reaction density, which causes undesirable bed aggregation (Rohatgi et al., 1982), and at $u/u_{mf} \geq 8$, the bed slugged in an uncontrollable mode, resulting in excessive silicon fines formation. Typically, u/u_{mf} of 3 to 5 is used for a normal operation.

Bed heights of 30.5, 45, and 61 cm were investigated to optimize the bed height. Based on the existing heater configuration, the 61 cm bed height was found to be the best of the three values to obtain a desirable temperature profile as shown in Figure 2, without wall deposit.

Two long-duration experiments were conducted: with 30% silane for 8 h, and with 50% silane for 5 h. In both cases, the reactor was operated without any sign of plugging the distributor. The mechanical feasibility of continuous withdrawal of particles to maintain a constant bed height was also demonstrated in these tests.

Silicon particle growth

In a fluidized bed, the reaction mechanism of silane pyrolysis can be described by a six-path process (Hsu et al., 1984a, b):

1. Heterogeneous deposition
2. Homogeneous decomposition
3. Coalescence
4. Coagulation
5. Scavenging
6. Heterogeneous growth on fines

Based on the above overall reaction model, this paper analyzes silicon particle growth on seed particles. Specifically, the large seed particles (e.g., more than 200 μm dia.) in an FBR sweep up and collect the homogeneously nucleated fines (e.g., smaller than 1 μm) onto the particle surfaces, followed by sealing via the heterogeneous deposition. The paper concentrates on describing particle growth aspects, whereas the reaction mechanism has been treated in an earlier publication (Hsu et al., 1984b). The silicon particle growth is approximated as the combination of growth due to scavenging of homogeneous fines and that due to heterogeneous chemical vapor deposition.

Consider a seed particle of radius r_1 traveling up and down in a fluidized bed. The surrounding environment contains homogeneously nucleated fines of weight concentration ω_f traveling at a velocity U' of the fluidizing gas. The mass balance around a particle due to the scavenging and incorporation of homogeneously nucleated fines is (Levenspiel, 1979)

$$\rho 4\pi r_1^2 dr_1/dt = \pi r_1^2 (\Delta U)\omega_f \tag{2}$$

where ΔU can be approximated by the actual fluidized gas velocity U'. ω_f can be approximated from the silane concentration and the subsequent concentration reduction in the coalescence step leading to the fines (Hsu et al., 1984b).

$$\omega_f = C_{Ao} \times M_{Si} \times \frac{k_g}{k_s + k_g} \times \frac{1}{1 + X_A} \times 0.5 \times \frac{25 \times 10^{-10}\,2}{0.15 \times 10^{-6}} \quad (3)$$

Silane feed conc. | Si mol. wt. | Homog. reaction fraction | Dilution factor due to hydrogen formation | Average in bed | No. of fines reduced from collisions of nuclei (50 Å) to fines (0.3 μm)

where X_A is the feed mole fraction of silane.

Equations 2 and 3 describe the concentration of homogeneously nucleated finds and their scavenge by the seed particles. The numerical factors in Eq. 3 correct for the average concentration of fines reduced from coalescence of 50 Å homogeneous nuclei to ~0.3 μm fines.

On the other hand, the seed particle growth due to heterogeneous deposition can be described by the following mass balance:

$$N \cdot 4\pi r_2^2\, dr_2/dt = \frac{k_s}{k_s + k_g} C_{Ao} M_{Si} u A \quad (4)$$

where

$$N = \frac{\omega_o}{\frac{4}{3}\pi r_o^3\, \rho} \quad (5)$$

N = number of particles in the bed
ω_o = initial bed weight
r_o = radius of the initial seed particle
u = superficial velocity of the gas, $\epsilon U'$

The total growth rate of a particle equals the sum of Eqs. 2 and 4. Based on Eqs. 2 and 4, the theoretical particle growth can be estimated as shown in Table 1. This modeling estimate can be compared with particle growth calculated from a mass balance over the experiment and measured particle size distribution of the product via sieve analysis. It can be seen that the estimate from the model agrees with the experimentally measured and calculated sizes. Combining Eqs. 4 and 5, the following relationship holds:

$$\frac{dr_2}{dt} = p \frac{r_o F}{\omega_o} C_{Ao} \quad (6)$$

where F is the total flow rate, uA, and p is a constant, $1/3\,(k_s/k_s + k_g)\rho M_{Si}$. The linear relationship is expected, as a first-order kinetics has been assumed for the heterogeneous chemical vapor deposition (CVD) reaction. This means that the heterogeneous deposition rate is linearly proportional to C_{Ao}, r_o, and F, and is inversely proportional to ω_o.

Equation 2 shows that the growth rate via scavenging of homogeneous fines also is linear with respect to the feed silane concentration. If r_o, F, and ω_o are held constant, a simple correlation of overall deposition rate dr/dt, (while $dr = dr_1 + dr_2$) vs. silane feed concentration, C_{Ao}, can reasonably be assumed. Furthermore, linear growth rates of different operating conditions can be compared with each other by normalizing the deposition rate data, μm/h, from Table 1 vs. initial particle size of 227 μm, initial bed weight of 400.2 mol silicon, and total flow rate of 3.0 mol/min. These rate data, dr/dt, are plotted against percentage silane feed mole fraction, X_A, in Figure 5. This results in a straight line correlation. In this way, the rate constant of the overall growth model, g, is obtained as 15 μm/h for the FBR design.

$$\left.\frac{dr}{dt}\right|_{r_o, \omega_o, F} = gX_A, \quad \text{where } dr = dr_1 + dr_2 \quad (7)$$

Performance of silicon withdrawal system

The purpose of the withdrawal tube is to selectively take large particles out of the bed in a continuous or semicontinuous fashion. This can be achieved with the withdrawal system sketched in Figure 3. The results on withdrawal performance are shown in Figure 6. Fifty percent of the particles in the withdrawal boot have particle sizes greater than 300 μm, while the average particle size in the bed is about 220 μm. If economically necessary, the undersized particles (after product particle screening) can be recycled to the reactor for further growth. If 10% of the bed particles are withdrawn, the distribution ratio of particles in the withdrawal system vs. that in the bed for 400 μm size is 1.4, whereas the distribution ratio of 1 stands for almost uniform distribution of bed particles toward the withdrawal boot. Thus, the

Table 1. Silicon Particle Growth Rates

			Theoretical						
					From Models			Est. from Mass Balance	
Silane Conc. vol. %	Run Duration min	Initial Dia. of Particle μm	Est. Deposition Due to Scavenging* μm	Est. Heterogeneous Deposition** μm	Dia. μm	% Dev. from Meas.	Meas. Final Dia. Size Anal. μm	Dia. μm	% Dev. from Meas.
20	90	227	4	5	236	0%	235.5	233	−1%
50	120	268	13	28	309	+3.7%	297.6	305	+2.5%
57	120	236	13	18	267	+5.9%	251.9	259	+2.8%
80	173	212	14	24	250	+3.5%	241.5	244	+1.1%

Average initial bed weight, 10 kg; T = 650°C, $U/U_{MF} = 5$
*Eq. 2
**Eq. 3

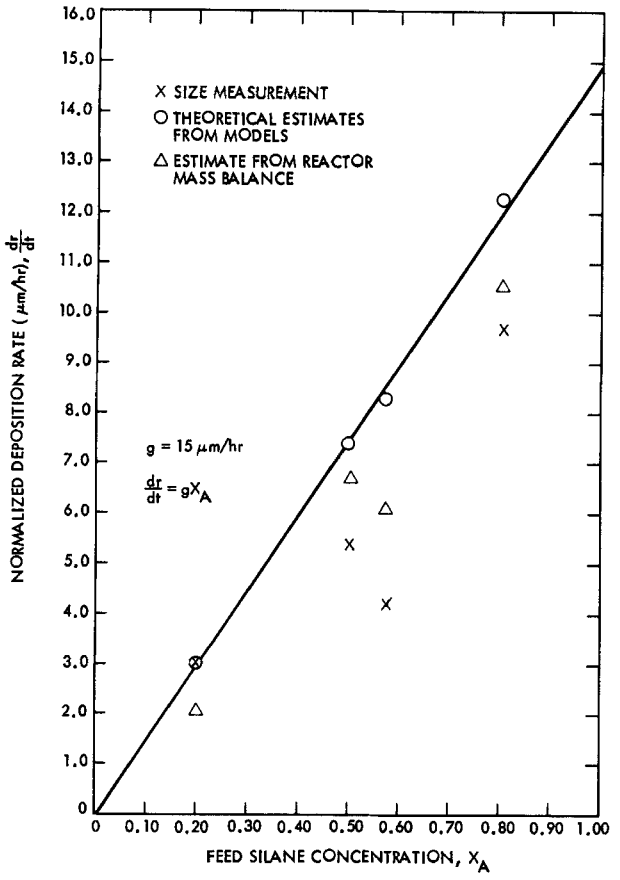

Figure 5. Normalized deposition rate vs. feed silane concentration.

selective withdrawal of larger particles in the mildly fluidized column is established.

Performance of jet milling device

The effectiveness of silicon grinding by the impingement of two opposing jets was studied with respect to nitrogen carrier

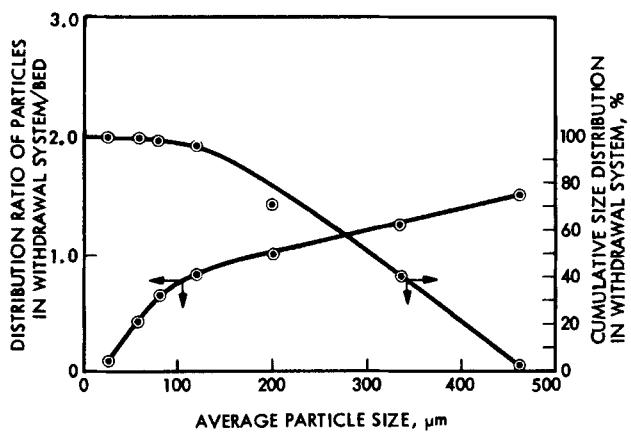

Figure 6. Performance of product withdrawal system on ratio of particle sizes in withdrawal system vs. bed.

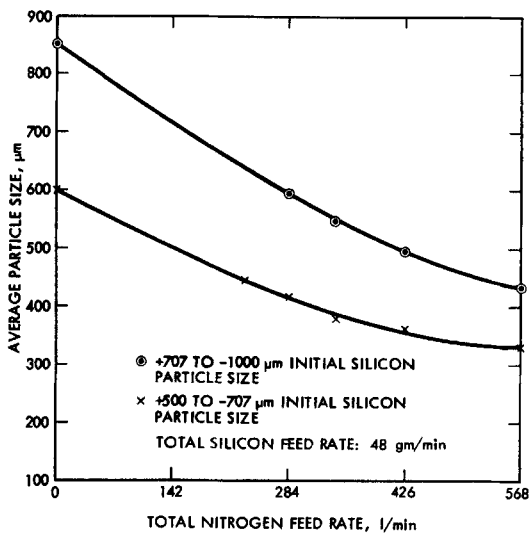

Figure 7. Effect of gas flow rate on particle size reduction via jet mill grinding.

flow rate with different initial silicon particle sizes. As shown in Figure 7, the average particle sizes of 600 and 850 μm (anticipated product sizes from a commercial reactor) were reduced to 330 and 430 μm, respectively, after one pass through at a nitrogen flow rate of 568 L/min and a silicon feed rate of 48 g/min. In another experiment, the one-pass yield for the desirable fraction of +75 to −355 μm range obtained from the feed size of +500/−707 μm is 15.8% at 340 L/min N_2 feed rate and 48 g/min silicon feed rate, whereas the two-pass yield increases to 28.3%. The effect of silicon feed rate is shown in Figure 8. As shown, beyond the 100 g/min silicon feed rate, further particle size reduction appears insignificant.

Performance of silicon cleaning device

To produce semiconductor-grade silicon particles it is necessary to start with clean silicon seed material. In a commercial system it is envisioned that only the first starting batch of seed

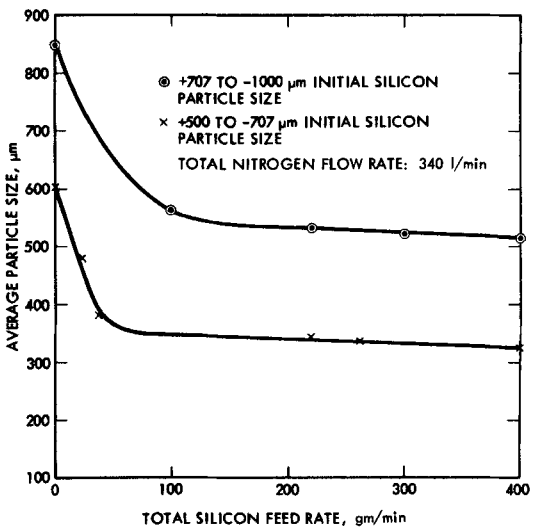

Figure 8. Effect of silicon feed rate on particle size reduction via jet mill grinding.

Table 2. Impurities in Material for Bed Particles

Elements	Raw Particles as Purchased	Jet-Milled, Acid-Cleaned Seed for FBR
P	0.2	0.2
Fe	20	≤0.6
Cr	0.05	0.03
Ni	10	<0.5
Cu	0.06	≤0.02
Zn	<0.02	≤0.04
Co	≤0.1	≤0.1
Mn	0.5	≤0.02
Na	≤0.1	≤0.1
Mg	≤1	<1
Al	2	0.05
S	<1	<1
K	≤0.07	<0.1
Ca	0.6	0.1

In ppma as determined by spark source mass spectroscopy

needs to be cleaned. Later on the FBR and fluid jet mill generate clean seeds. For this reason, silicon particles of less than 2 mm dia. were purchased from Dynamit Nobel with a minimum impurities level as indicated in Table 2. These particles are reduced to 200 to 300 μm dia. by employing the seed-particle generation device and then are cleaned in the JPL-developed fluidized-bed silicon cleaning device.

The cleaning of silicon seed obtained from grinding of silicon chucks includes the following steps:

1. Deionized water wash in a liquid-solid fluidized-bed mode to remove fine silicon particles of less than 75 μm dia.
2. Seed cleaning in a mixture of two parts 12N HCl, one part 16N HNO_3 in fluidized-bed mode for 20 min.
3. Acids drained and particles washed with deionized water in fluidized-bed mode until the effluent water is neutral.
4. Etching of silicon particle with 48% HF in a fluidized-bed mode for 20 min.
5. HF drained and particles washed with deionized water in a fluidized-bed mode until effluent water is neutral and has a resistivity of 16 megaohms.
6. Wet particles dried in a diffusion furnace at 150°C under nitrogen blanket.

Table 4. Purity of Product from Fluidized-Bed Reactor with Quartz Liner

Elements	Jet-Milled, Acid-Cleaned Seed for FBR	FBR Product*
P	0.2	0.1
Fe	≤0.6	≤0.6
Cr	0.03	<0.02
Ni	<0.5	<0.5
Cu	≤0.02	<0.02
Zn	≤0.04	<0.04
Co	≤0.1	≤0.1
Mn	≤0.02	<0.02
Na	≤0.1	≤0.1
Mg	1	<1
Al	0.05	0.05
S	<1	<1
K	<0.1	<0.1
Ca	0.1	0.1

Analysis in ppma as determined by spark source mass spectroscopy conducted by Northern Analytical Lab
*Run Nos. 502 and 503

7. After drying, particles transferred into a plastic bag and sealed.

As indicated by the following equations, the mixture of HNO_3 and HCl will remove metallic impurities as soluble chlorides:

$$Fe \rightarrow Fe^{+3} \text{ (oxidation by } HNO_3)$$

$$Fe^{+3} + 4HCl \rightarrow FeCl_4 \text{ (soluble)} + 4H^+$$

The silicon oxide layer coating on the particles is removed by etching with concentrated HF.

$$Si + 2HNO_3 \rightarrow SiO_2 + HNO_2$$

$$SiO_2 + 4\,HF \rightarrow SiF_4 \text{ (gas)} + 2H_2O$$

The acid-cleaned particles have impurity levels below the detection limits of the spark source mass spectroscopy analytical technique, as shown in Table 2.

Table 3. Purity of Product from Fluidized-Bed Reactor without Quartz Liner

JPL Run No.	Cr	Fe	Ni	Co	Mo	W	Na	Total Identified
111 (Seed)	4	—	1	—	0.05	0.04	1.3	—
111-4P*	16 (15%)	77 (72%)	11 (11%)	0.16	0.76 (0.7%)	0.1	2	107
111-8P**	45 (17%)	185 (70%)	31 (12%)	0.36	3.8 (1.4%)	0.15	1.3	266
115P†	46 (17%)	197 (71%)	30 (11%)	0.4	1 (0.4%)	0.1	1.1	275
115 Ingot, bottom	0.7	—	—	—	—	—	1.3	—
115 Ingot, middle	0.2	—	—	—	—	—	4.2	—
115 Ingot, top	0.3	—	—	—	—	—	1.2	—

Product analysis in ppmW via neutron activation analysis, Lawrence Livermore Laboratory
Reactor wall material, stainless steel 316: Cr 17%, Fe 70%, Ni 12%, Mo 2.5%, Mn 2%, Si 1%
For experimental conditions for runs 111 and 115, see Hsu (1985)
*4P, product obtained after 4 h
**8P, product obtained after 8 h
†P, final silicon product

Performance of quartz liner

The performance of a quartz liner mounted inside the stainless water reactor was evaluated based on the following criteria:

1. The time required to reach a steady state bed temperature of 650°C when an 11 kg batch of 250 μm avg. dia. silicon particles is fluidized with hydrogen at a U/Umf ratio of 4.

2. The maintenance of the proper bed-temperature profile necessary to eliminate deposition of silicon on the inside quartz liner wall. If this parameter is not properly established, the quartz liner will break during thermal cycling due to the differential thermal expansion between quartz and silicon.

It takes approximately 3 h to reach the steady state bed temperature of 650°C. This is about 1 h longer than is required if silicon is directly heated through the stainless steel wall (no quartz liner). Once the required bed temperature is reached however, its maintainability is fairly good.

Product purity

The purity of the FBR product was determined for two cases:

1. The FBR was operated without a liner, so that silicon particles were exposed to the hot stainless steel reactor wall.

2. The FBR was operated with a quartz liner that isolated the silicon particles from the stainless steel reactor wall.

For the no-liner case, the concentrations of metallic impurities in the FBR product are shown in Table 3. These data indicate that the silicon product is heavily contaminated with metallic impurities. The iron, chromium, and nickel impurities are approximately 70, 17, and 12% of the total identified impurities. These proportions are similar to the composition of the stainless steel 316 reactor wall material. It is evident, therefore, that hot silicon particles physically removed the stainless steel wall materials and that the metallic impurities are incorporated onto the seed silicon during the silane pyrolysis.

For the case with the quartz liner, the metallic impurities in the FBR product are shown in Table 4. The use of a quartz liner as a barrier between the silicon particles and the stainless steel reactor wall helped to eliminate metallic contamination in the product silicon during fluidized-bed processing. The metallic impurities in the product silicon generally are less than the detection capability limits of spark source mass spectroscopy. An improved analytical technique that can repeatedly and directly detect most heavy metal, B- and p-elemental impurities in the ppb range is very much needed. The purity of the deposited layer of silicon is equal to or better than that of the starting silicon seed material.

Conclusions

A 15 cm dia. fluidized-bed reactor was demonstrated to be capable of producting 3.5 kg/h of silicon using 80% silane feed concentration. The longest duration demonstrated was 8 h of operation, during which time the product was semicontinuously withdrawn from a mildly fluidized column at the bottom of the reactor. The fines collected at the effluent filter were less than 10% of the silicon in the silane feed. Also, a contamination-free seed generation method via jet milling of silicon particles was developed. In this work, theoretical estimates of silicon particle growth based on heterogeneous deposition and scavenging mechanisms agreed well with experimental size measurements.

Acknowledgment

This work was sponsored by the U.S. Department of Energy, through an agreement with the National Aeronautics and Space Administration. The authors would like to thank Donald Feller and James Lloyd for valuable laboratory assistance.

Notation

A = cross-sectional area of the fluidized bed, cm^2
C_{Ao} = feed silane concentration in molar units
Cp_1 = specific heat of silane, kcal/mol · °C
g = linear particle growth rate constant, μm/h
ΔHr = heat of reaction, kcal/mol
K_g = first-order rate constant for homogeneous decomposition of silane, 6.6 s^{-1} at 650°C [average of 7.1 s^{-1} Newman et al. (1979) and 6.1 s^{-1} Purnell and Walsh (1966)]
K_s = first-order rate constant for heterogeneous decomposition of silane, 4.8 s^{-1} at 650°C (Farrow, 1974)
M_{Si} = molecular weight of silicon
N = number of particles in bed
Q_H = minimum power required for the heater, kcal/min
Q_W = rate of energy removal from distributor plate by cooling, kcal/min
r = particle radius
Δr_1 = linear growth of particle radius via scavenging of homogeneous fines
Δr_2 = linear growth of particle radius via heterogeneous CVD
T = temperature, K
t = time
u = superficial velocity of gas
ΔU = difference between gas and solid velocities
U' = actual velocity of fluidizing gas
X_A = mole fraction of feed silane
ρ = density of silicon particles
ϵ = void fraction of fluidized bed
ωf = weight concentration of homogeneously nucleated fines
η_1 = flow rate of silane, mol/min

Literature cited

Farrow, R. F. C., "The Kinetics of Silicon Deposition on Silicon by Pyrolysis of Silane," *J. Electrochem. Soc., Solid-State Sci. Tech.*, **121** (7), 899 (1974).

Hogle, R., G. Hsu, and R. Lutwack, "In-house Study—Fluidized-Bed Silane Pyrolysis," JPL Low-Cost Solar Array Proj. Rept. No. 5105-89 (1978).

Hsu, G. C., "Fluidized-Bed Development at JPL," *Proc. Flat-Plate Solar Array Proj. Workshop, Los-Cost Polysilicon for Terrestrial Photovoltaic Solar-Cell Applications,* DOE/JPL Rept. 5101-287, p. 147, Las Vegas (Oct., 1985).

Hsu, G., R. Hogle, N. Rohatgi, and A. Morrison, "Fines in Fluidized-Bed Silane Pyrolysis," *J. Electrochem. Soc.*, **131** (3), 660 (Mar., 1984a).

Hsu, G., A. Morrison, N. Rohatgi, R. Lutwack, and T. McConnell, "Fluidized-Bed Silicon Deposition," 17th IEEE Photovoltaic Spec. Conf., Kissimmee, FL (May, 1984b).

Kunii, D., and O. Levenspiel, *Fluidization Engineering,* Wiley, New York (1969).

Lackey, W. J., and J. D. Sease, "Means for Effecting Fluidization in Pyrolytic Carbon Coating," U.S. Pat. No. 3,889,631 (June 17, 1975).

Levenspiel, O., *The Chemical Reactor Omnibook,* Oregon State Univ. Bookstore (1979).

Newman, C. G., H. E. O'Neal, M. A. Ring, F. Leska, and N. Shipley, "Kinetics and Mechanism of the Silane Decomposition," *Int. J. Chem. Kinetics,* **11,** 1167 (1979).

Purnell, J. H., and R. Walsh, "The Pyrolysis of Monosilane," *Proc. Roy. Soc.*, **293A,** 543 (1966).

Rohatgi, N., and G. Hsu, "Silicon Production in a Fluidized-Bed Reactor: A Parametric Study," Rept. 5101-248 (JPL Pub. D-1283). (Oct., 1983).

Rohatgi, N., G. Hsu, and R. Lutwack, "Silane Pyrolysis in a Fluidized-Bed Reactor," *Electrochem. Soc. Symp. Proc.*, Montreal, 477 (1982).

Manuscript received June 6, 1985, and revision received July 2, 1986.